

Electron scattering at 180° from the "single-hole" states in ^{15}N

R. P. Singhal

Kelvin Laboratory, Department of Natural Philosophy, University of Glasgow, Glasgow, Scotland

J. Dubach, R. S. Hicks, R. A. Lindgren, B. Parker, and G. A. Peterson

Department of Physics and Astronomy, University of Massachusetts, Amherst, Massachusetts 01003

(Received 20 December 1982)

Results are presented for the scattering of electrons through 180° from the $\frac{1}{2}^-$ ground state and the $\frac{3}{2}^-$ excited state at 6.32 MeV in ^{15}N . The range of the momentum transfer q is from 0.70 to 3.25 fm^{-1} . Comparisons are made with the predictions of the $0p$ -shell proton-hole model, a large basis $2\hbar\omega$ shell model calculation, and core polarization models. In general, it was found that the theoretical description of the data improved markedly as the model space was expanded, but the predicted cross sections were consistently below the data for $q > 2.4 \text{ fm}^{-1}$. The present data rule out the low value of the Migdal parameter g' needed to describe the (e,e') data for ^{12}C and ^{13}C , and do not support the previous suggestion that pion-condensation effects are important in finite nuclear systems.

NUCLEAR REACTIONS $^{15}\text{N}(e,e')$, $E=70\text{--}327 \text{ MeV}$, $\theta=180^\circ$, measured $\sigma(E,\theta)$ for ground, 6.32 MeV levels. ^{13}C deduced transverse form factors. Comparisons with models.

I. INTRODUCTION

In the past few years the availability of good quality electron scattering $M1$ form factors has generated sustained theoretical interest. The experimental results generally show prominent deviations from the predictions of conventional nuclear structure calculations for momentum transfers $q \geq 2 \text{ fm}^{-1}$. Conventional descriptions of the nucleus only in terms of nucleonic degrees of freedom are questionable at such high momentum transfers, and other processes, such as meson exchange currents (MEC), need to be considered.¹ Even then serious discrepancies remain. Subsequent attempts to explain the new data have led to the infusion of new and sometimes exotic effects into the realm of conventional nuclear structure physics. For example, pion-condensation effects² have been predicted to have a strong influence on magnetic dipole transitions at momentum transfers around 2 fm^{-1} . However, this idea and others have met with controversy.

In this paper, we present results of a measurement of 180° electron scattering from the nucleus ^{15}N . In the zeroth order the ground state of ^{15}N may be thought of as a $0p_{1/2}$ proton hole in a doubly-closed $0p$ shell. For instance, the experimental value of the magnetic dipole moment of the ^{15}N ground state is $-0.283 \mu_N$, and compares well with $-0.263 \mu_N$, the value for a $0p_{1/2}$ proton hole. The $\frac{3}{2}^-$ state at 6.32 MeV is then formed by the substitution of a $0p_{3/2}$ proton hole for the $0p_{1/2}$ proton hole. Any discrepancies between the experimental electron-scattering form factors and the single proton-hole description of these two states should be interpreted in terms of a contribution from multi- $\hbar\omega$ configurations and/or the effects of non-nucleonic degrees of freedom, e.g., MEC. There is already some evidence³ that additional configurations significantly dilute the single-hole nature of these states, and as

we shall see, calculations assuming single-proton holes fail to explain the data reported here.

The effects of multi- $\hbar\omega$ configurations may be studied by performing shell-model calculations in an extended basis space. For ^{15}N we have considered the role of $2\hbar\omega$ configurations with two particles in the $1s0d$ shell. Excitations from the $0s$ shell and to the $1p0f$ shell were also considered. Other techniques for evaluating these core-polarization effects are performed by the use of perturbation theory.⁴ For example, the calculations of Suzuki *et al.*⁵ consider up to $12\hbar\omega$ excitations and predict important modifications of the strength and shape of the electron scattering form factors. Delorme *et al.*² include core polarization to all orders by constructing an effective spin operator which can be used in the restricted model space of the $0p$ shell. The particle-hole and the Δ -hole interactions responsible for the polarization effects are described by the exchange of π and ρ mesons. An additional short-range repulsion whose strength is defined by the Migdal parameter g' is also included. From an analysis of the $M1$ form factors of ^{12}C and ^{13}C , Delorme *et al.*² obtain $g'=0.44$ which opens the possibility of observing the precursor of pion condensation, sometimes called precritical opalescence, in nuclei. Suzuki *et al.*⁶ have questioned some of the assumptions in the work of Delorme *et al.*,² but both groups have stressed the need for studying ^{15}N elastic magnetic cross sections.

In the following, we first discuss the experimental details and then compare the various theoretical predictions with the data.

II. EXPERIMENTAL DETAILS

The experiment was performed at the MIT-Bates Electron Linear Accelerator Laboratory using the 180° scatter-

ing facility.⁷ Gaseous ^{15}N of 99.2% isotopic purity was used in a target cell at room temperature. Incident and scattered electrons traveled parallel to the axis of the target cell, a stainless steel cylinder of radius 3.81 cm and length 11.43 cm. The entrance and exit windows were made of stainless steel of thickness $25\ \mu\text{m}$ and were sealed to the target cylinder by rubber *O* rings. The target temperature was stabilized by a flow of compressed air through copper tubing in good thermal contact with the target exterior. During data collection, the target was sealed and the target temperature and pressure were monitored continuously by means of a platinum resistance thermometer and a pressure transducer. During four separate sessions of data collection, the computed leak rate was less than 0.1% per day. After each data collection session, ^{15}N gas was recovered by absorption over charcoal cooled by liquid N_2 . Proton elastic cross sections⁸ for absolute normalization were measured by using an identical second target filled with hydrogen. Typical target thicknesses varied from 19 to $113\ \text{mg cm}^{-2}$ for ^{15}N and from 2 to $4\ \text{mg cm}^{-2}$ for ^1H .

The momentum-dispersed beam spot was approximately $2 \times 30\ \text{mm}^2$ in the form of a vertical line. This diffuse beam spot reduced the severity of beam heating effects on gas target density. Such effects were studied for the case of ^{14}N by varying the average current from 5 to $25\ \mu\text{A}$ in $5\ \mu\text{A}$ steps at an incident electron energy of 90 MeV. The count rate in the elastic peak of ^{14}N decreased linearly with increasing beam currents, resulting in a 1% loss of target thickness for energy $5\ \mu\text{A}$ increase in beam current. The maximum beam current used in the present measurements was $32\ \mu\text{A}$.

The solid angle was defined by a rectangular aperture whose horizontal and vertical dimensions could be adjusted. For most measurements the aperture was fixed at 5.08 (horizontal) \times 25.4 (vertical) cm^2 , corresponding to a solid angle of 3.51×10^{-3} sr. Only below 100 MeV, where the contribution of the Coulomb scattering is significantly increased, did we reduce the aperture to $5.08 \times 7.62\ \text{cm}^2$.

For 180° scattering the stainless steel windows of the gas target also contributed to the observed count rate. In the case of hydrogen, the recoil energy for the proton is very large, and the elastic peak sits on a continuum spectrum which is due to the various elements in the window material. However, for ^{15}N the recoil energy is not so large, and the underlying background may have some structure. Therefore, the contribution of the stainless steel foils under the ^{15}N elastic peak was measured by using the hydrogen gas cell at spectrometer field settings for the ^{15}N elastic peak. For energies greater than 100 MeV, the window contribution was insignificantly small for the ^{15}N elastic peak because most elements in stainless steel have 0^+ ground states and do not contribute to the magnetic scattering. The background contribution was only noticeable at lower energies where the Coulomb scattering cross sections increase rapidly.

At energies below about 100 MeV the contribution of the Coulomb scattering from ^{15}N itself is more important than the foil background. Due to the finite angle of acceptance and multiple scattering in the target, electrons scattered at angles other than 180° are counted by the spectrometer detection system. In our measurements the effective scattering angle varied from 177.8° to 179.0° .

The Coulomb contribution to the elastic scattering was calculated from the published charge distribution parameters⁹ for ^{15}N by using a phase-shift code. This method was followed for incident electron energies E_0 above 95 MeV. For $E_0 = 80$ MeV, the effective scattering angle was calibrated by measuring elastic Coulomb scattering from ^{20}Ne , and for $E_0 = 90$ MeV, cross sections for ^{14}N were used.

The reduction of the data to obtain experimental cross sections followed a standard technique.¹⁰ The cross sections for the ground state and 6.32 MeV state are listed in Table I. For most runs the maximum excitation energy studied was approximately 30 MeV. The data on other states will form the subject of future publications.

III. INTERPRETATION OF THE DATA

A. General

In order to account for Coulomb distortion effects, the data have been plotted as a function of an effective momentum transfer

$$q_{\text{eff}} = q \left[1 + f_c(E) \frac{Z\alpha\hbar c}{ER_m} \right].$$

By comparing plane-wave Born-approximation form factors with those calculated in the distorted-wave Born approximation, it was found that

$$f_c(E) = 0.920 + 0.001E\ \text{MeV}$$

for $R_m = 2.705\ \text{fm}$.

In Figs. 1 and 2 we present the comparison of the exper-

TABLE I. Form factors deduced from the experimental cross sections.

| Incident electron energy (MeV) | $ F_T ^2 = \sigma/\sigma_0^a$ ($\times 10^6$) | |
|--------------------------------------|---|---|
| | $E_x = 0.00\ \text{MeV}$ $J^\pi = \frac{1}{2}^-$ | $E_x = 6.32\ \text{MeV}$ $J^\pi = \frac{3}{2}^-$ |
| 70.4 | | 125. (5) |
| 80.2 | 41. (9) | 134. (5) |
| 89.6 | 58. (11) | 135. (5) |
| 94.9 | 89. (8) | 120. (6) |
| 99.3 | 90. (10) | 117. (6) |
| 109.4 | 125. (6) | 141. (5) |
| 119.5 | 143. (4) | 144. (6) |
| 129.5 | 174. (5) | 176. (5) |
| 149.6 | 159. (4) | 168. (6) |
| 169.4 | 134. (5) | 150. (5) |
| 189.2 | 88. (4) | 98. (7) |
| 208.9 | 49. (7) | 66. (6) |
| 224.2 | 30. (9) | 34. (10) |
| 239.1 | 20. (7) | 22. (7) |
| 273.4 | 6.8(12) | 4.4 (13) |
| 297.8 | 3.0(21) | 1.6 (21) |
| 326.7 | 1.1(25) | 0.34(46) |

^a

$$\sigma_0(\theta = 180^\circ) = \left[\frac{Z\alpha\hbar}{2k_1} \right]^2 \left[1 + \frac{2k_1}{AMc} \right]^{-1};$$

k_1 is the incident electron momentum and M is the nucleon mass. The numbers in parentheses are percentage errors.

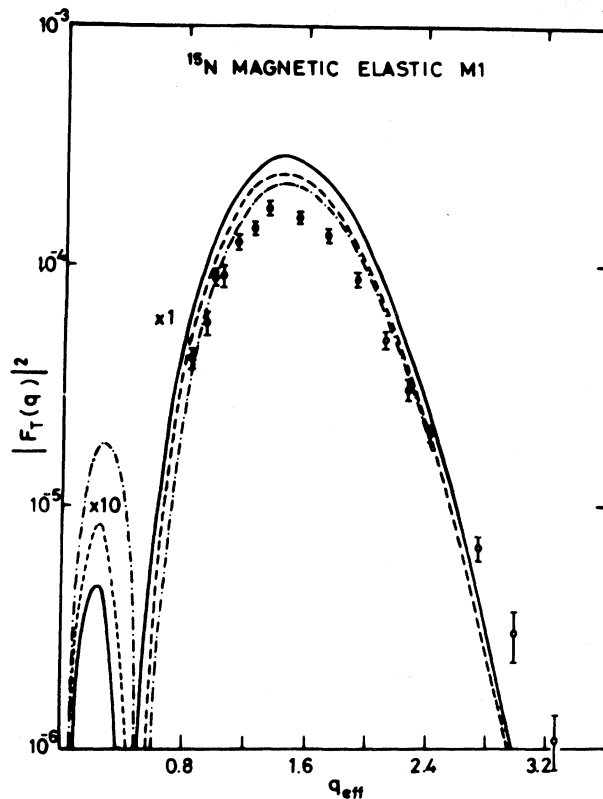


FIG. 1. The transverse form factor for elastic $M1$ scattering from ^{15}N is shown as a function of q_{eff} in fm^{-1} . The data are from Table I and the continuous (dashed) curves are predictions for a $0p_{1/2}$ proton hole with (without) meson-exchange-current effects for $b = 1.70$ fm. The dotted-dashed curve shows the results of a $2\hbar\omega$ shell model calculation including MEC effects. The MEC contributions are about equal for the $0p$ -proton hole and the shell model calculations.

imental data with the single-proton-hole form factors calculated with harmonic oscillator wave functions using a size parameter $b = 1.70$ fm. This value reproduces the charge radius of ^{15}N . The nucleon finite size and the shell model center-of-mass corrections were made in the standard fashion.¹¹ In both cases, the calculated form factors appreciably exceed the experimental values except at high q , where the predictions decrease rapidly. This is similar to the high- q discrepancies observed for other $M1$ transitions in the $0p$ shell nuclei.¹² A renormalization of the calculated form factors could improve agreement with the data at medium momentum transfers but will exacerbate the high- q discrepancy. The photon point ($q = E_x/\hbar c$) values will also be less well predicted. Thus there seems to be no advantage to be gained by a straightforward renormalization of the nucleon magnetic moments. This is similar to the case of the longitudinal form factor¹³ in the excitation of the 6.32 MeV state of ^{15}N , where a constant effective charge fails to reproduce the q dependence of the experimental form factor.

We have calculated the effects of one-pion exchange currents following the procedure of Ref. 1. The contributions of the pair, pionic, and the nucleon-resonance terms

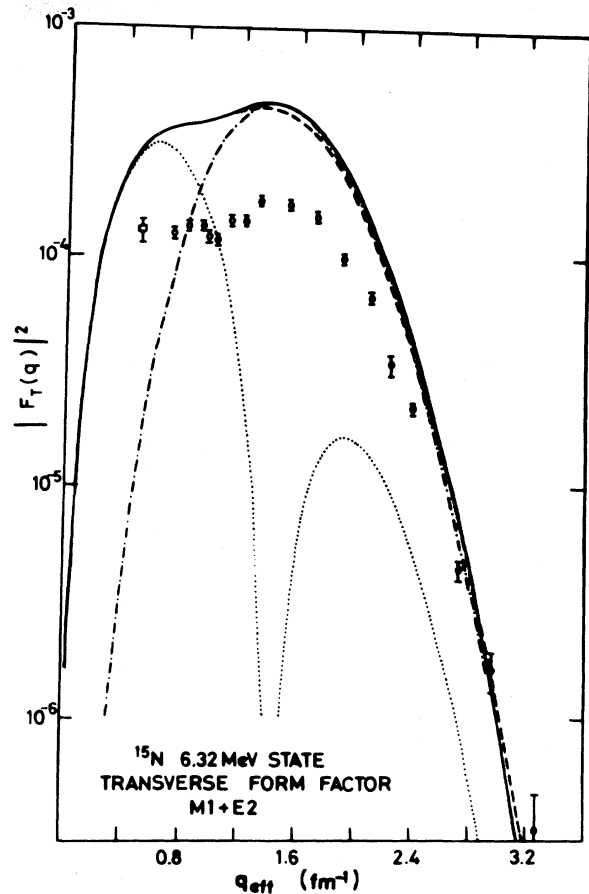


FIG. 2. The transverse form factor for the excitation of the 6.32 MeV, $\frac{3}{2}^-$ state in ^{15}N . Results of the present measurements are represented by circles. The square shows a lower- q point measured by Beer *et al.* (Ref. 14). The continuous (dashed) curves are predictions for a $0p_{1/2}$ - $0p_{3/2}$ proton hole transition with (without) MEC effects for $b = 1.70$ fm. The contributions of the $M1$ (dotted line) and the $E2$ (dotted-dashed line) multipoles are also shown.

were evaluated. The results are also presented in Figs. 1 and 2. These MEC terms increase the calculated form factor for the ground state by 20% over a large range of momentum transfers, but do little to improve the agreement with the shape of the experimental form factors. The effect of MEC on the form factor for the 6.32 MeV state is small and cannot account for the discrepancy between the data and the one-body calculations. It is noted that at $q \sim 2.8 \text{ fm}^{-1}$, the MEC contribution goes to zero because of a cancellation between the nucleon resonance and the pion and the pair contributions.

The position of the maximum in both form factors appears to be calculated correctly, and this indicates that the choice of the radial scale parameter, $b = 1.70$ fm, is realistic. In fact, we shall see later that even by removing all constraints on radial dimensions, nucleon magnetic moments, etc., it is not possible to obtain a good description of the $M1$ elastic form factor within the restrictions of the $0p$ shell.

Recent measurements of $(e, e'p)$ cross sections³ for ^{16}O indicated about 60% occupancy for the $0p_{1/2}$ ($0p_{3/2}$) proton hole in the ground (6.32 MeV) state of ^{15}N . Thus, significant deviations of the measured form factors of these states from the predictions of the single proton hole model may be expected. In order to investigate the role of configurations outside the $0p$ shell, we discuss the results of several theoretical calculations.

B. The shell model

After the $0p$ proton holes, the contribution of the $2\hbar\omega$ configurations may be expected to provide the next most important component in the description of the ^{15}N ground and 6.32 MeV states. The effects of such configurations were evaluated by means of a shell model calculation which included $2\hbar\omega$ excitations within the basis space of $0s$ to $0f1p$ shells. This allows the following configurations: $0p^{-1}$; $0s^{-1}0p^{-1}(1s0d)^1$; $0p^{-2}(0f1p)^1$; $0p^{-3}(1s0d)^2$. Following the procedure of Dubach and Haxton,¹⁵ the effective interactions used were those of Cohen-Kurath¹⁶ for the $0p$ shell, of Millener-Kurath¹⁷ for the $0p$ to $1s0d$ cross-section transition, and of Kuo¹⁸ for the $1s0d$ shell. The relative energy of the $0p$ and $1s0d$ shells was adjusted to obtain a good description of the level structure in ^{15}N . The calculational technique was similar to that described in the work of Whitehead *et al.*¹⁹

The shell-model calculation predicts a significant depletion, approximately 40%, of the single-hole configuration in the $\frac{1}{2}^-$ and $\frac{3}{2}^-$ states. This is consistent with the results of the $(e, e'p)$ experiment,³ although in light-ion transfer reactions we often find somewhat less depletion.²⁰ It is possible to change the admixture of the $2\hbar\omega$ configurations by adjusting the relative energy of the $0p$ and $1s0d$ shells, but this will diminish the quality of the predicted energy level scheme.

The shell-model wave functions predict a ground state magnetic dipole moment equal to $-0.363 \mu_N$, which is significantly larger than the experimental value of $-0.283 \mu_N$. The inclusion of the MEC effects improves the prediction by 3.4%, giving $-0.351 \mu_N$. Similarly, the calculated $B(M1\uparrow)$ value for the excitation of the 6.32 MeV state is $0.0384 e^2\text{fm}^2$, to be compared with $0.0229 \pm 0.0023 e^2\text{fm}^2$ measured in a resonance fluorescence experiment.²¹ Although a 20% reduction in the nucleon magnetic moments would give agreement for the photon point properties, comparison is made with form factor calculations which employ bare nucleon magnetic moments. The shell model calculations do not specify the radial shape of the single particle wave functions, and again we have used harmonic oscillator orbitals with the oscillator parameter $b = 1.70$ fm. The results are presented in Figs. 1 and 3.

For the $M1$ elastic form factor, the shell model results, which include the MEC corrections, give improved agreement with the data around the second maximum, but still underestimate the data at higher q . As shown in Fig. 3, the calculated form factor for the 6.32 MeV excitation is generally too large, with both the $M1$ and $E2$ multipoles being overestimated. Nevertheless, the shell model result represents a clear improvement over the pure single-hole calculation shown in Fig. 2. The discrepancy at high q , although smaller than in the case of the ground state, is again present.

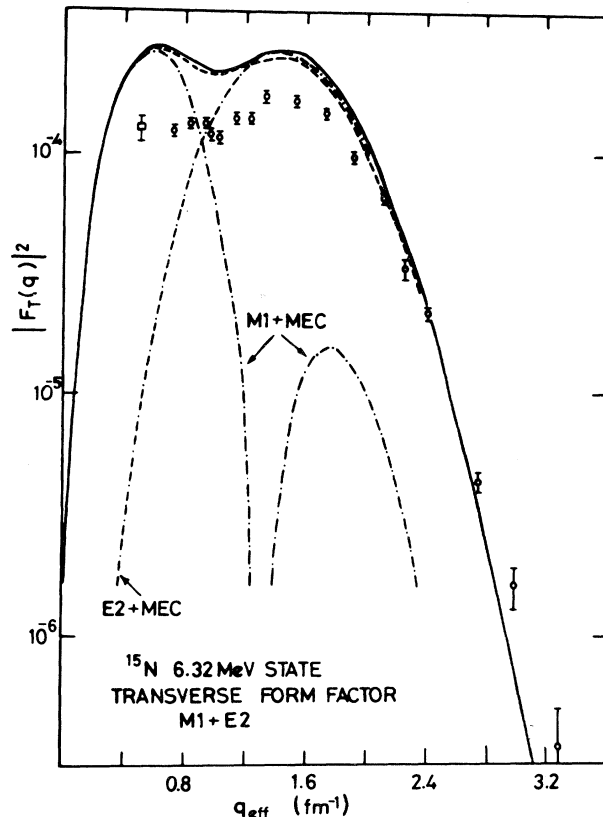


FIG. 3. Same as Fig. 2 but the curves are obtained from the $2\hbar\omega$ shell model calculations described in the text. The continuous (dashed) lines show the results with (without) MEC.

C. Core-polarization calculations

While the shell model emphasizes the role of $2\hbar\omega$ configurations, higher-lying configurations might also contribute significantly to the magnetic transitions in the $0p$ shell nuclei. This has been suggested by several core-polarization calculations^{2,5,22} that have been performed for $M1$ transitions in selected $0p$ shell nuclei. These calculations, which begin with unperturbed wave functions derived from the Cohen-Kurath interaction,¹⁶ have followed a wide variety of approaches to the problem. For example, in addition to the particle-hole and Δ -hole interactions, Delorme *et al.*² have considered a short range repulsion fixed by the Migdal parameter g' . Also included were one pion exchange currents generated by the pair term and the pionic term. The predicted $M1$ form factors in ^{12}C and ^{13}C improve considerably, but the required value of g' , 0.44, is considered to be too small.²³ Figure 4 shows the results of a similar core polarization calculation²⁴ for the magnetic $M1$ form factor in ^{15}N . It is obvious that the experimental data exclude values of $g' \leq 0.5$ and the preferred value of $g' \approx 0.6$ is consistent with the accepted value.²³ The ^{15}N magnetic elastic form factor is considered to be the appropriate candidate^{2,5} for a definitive study of the core-polarization effects by the techniques used by the Lyon group,² and the present results do not support the low values of g' obtained in Ref. 2 for ^{12}C

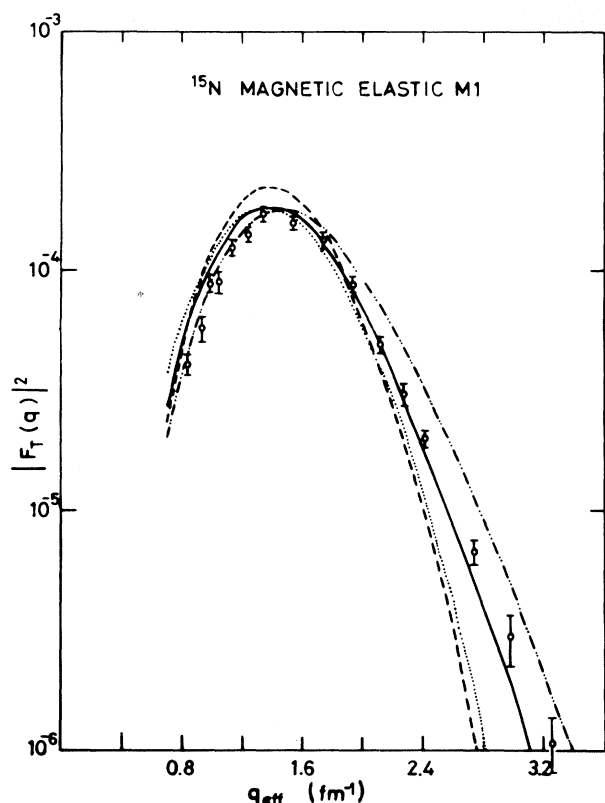


FIG. 4. Results of a core-polarization calculation (Ref. 24) by the Lyon group are compared with the magnetic elastic data for ^{15}N . The dashed curve is the single $0p_{1/2}$ proton-hole result. The effects of various choices of the Migdal parameter g' are shown by the other curves for which contributions of the pair and pionic exchange currents are also included ($-\cdot-\cdot-\cdot$ — $g'=0.5$, ——— $g'=0.6$, \cdots $g'=0.7$).

and ^{13}C magnetic dipole transitions.

Following a different approach, Suzuki *et al.*⁵ employed first-order perturbation theory with phenomenological interactions consisting of central and tensor parts. In the cases of the ^{13}C ground state, this procedure led to an improved description of the data for magnetic dipole scattering. The results of similar calculations for the ^{15}N elastic $M1$ form factor are shown in Fig. 5. The second maximum at $q \sim 1.4 \text{ fm}^{-1}$ is reduced by core polarization mainly due to the tensor force. The form factor at large q is enhanced by both core polarization and exchange currents. Although exact agreement is not obtained, these calculations do modify the single-hole form factor in the correct sense.

Suzuki's calculations⁴ for the 6.32 MeV, $\frac{3}{2}^-$ transition are shown in Fig. 6. In these calculations, $2\hbar\omega$ excitations were computed in the random phase approximation (RPA) with an effective interaction calculated from the Reid soft-core potential. The contributions of 4–12 $\hbar\omega$ excitations were estimated in perturbation theory, and pionic and pair exchange currents were included. Second-order effects due to the tensor interactions resulted in a substantial reduction from the single-hole predictions for both the

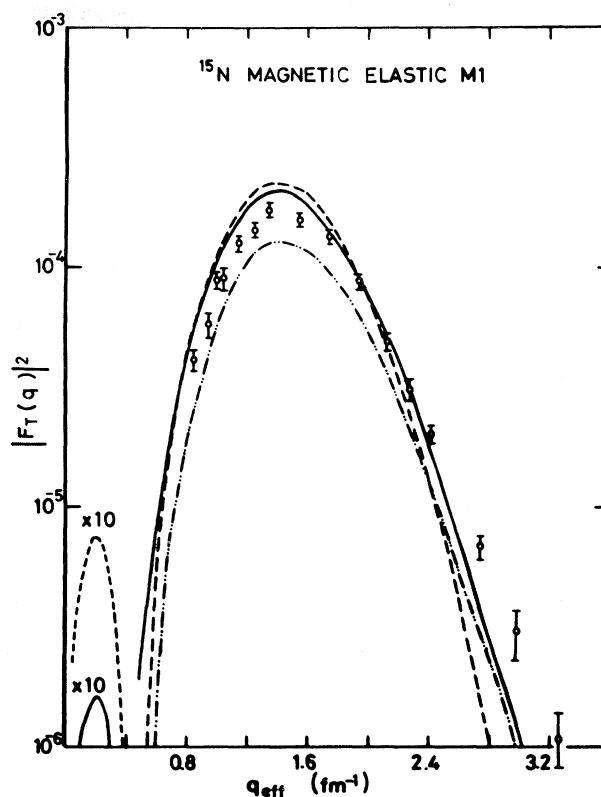


FIG. 5. The magnetic elastic form factor for ^{15}N is compared with the results of core-polarization calculations (Ref. 5) that include central and tensor interactions. The dashed curve is for a $0p_{1/2}$ proton hole with $b = 1.75 \text{ fm}$. The effect of core polarization due to the tensor interaction is to reduce the height of the calculated form factor over a large range of q as shown by the dashed-dotted curve. The continuous line represents the results of the full calculation with the central and tensor interactions and includes the contributions of the pair and pionic exchange currents.

$M1$ and $E2$ form factors. From Fig. 6, we observe that this core-polarization calculation describes the experimental data well, at least up to 2.4 fm^{-1} .

Finally, we note that lowest-order perturbation theory has also been utilized²⁵ to evaluate the core polarization contributions to the longitudinal $C2$ component of the 6.32 MeV form factor.¹³ By the inclusion of $2\hbar\omega$ and $4\hbar\omega$ excitations, Horikawa *et al.*²⁵ found that the $C2$ form factor could be increased by 35–55% at low momentum transfers. Core polarization effects on longitudinal form factors are primarily of isoscalar character. Since it is the isovector operator which provides the dominant contribution to most transverse form factors, transverse measurements are sensitive to an aspect of core polarization not strongly manifested in the longitudinal form factors.

D. Analysis of the magnetic elastic scattering using a phenomenological model

In this subsection we use a phenomenological model in which the form factor is expanded in powers of q^2 to

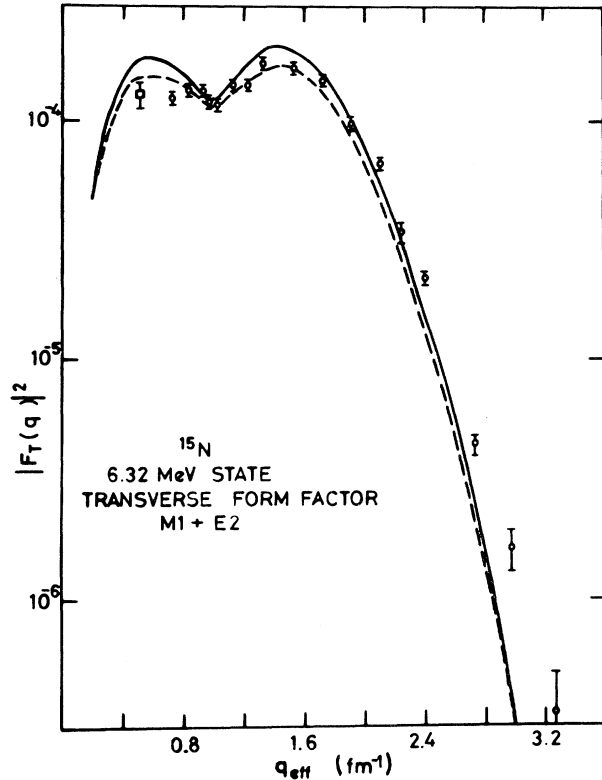


FIG. 6. The transverse form factor for the 6.32 MeV transition is compared with the predictions of core-polarization calculations (Ref. 4). The experimental data are from the present work (circles) and from Ref. 14 (square). For the solid curve the effects of $2\hbar\omega$ configurations were treated in RPA and 4–12 $\hbar\omega$ configurations were treated in perturbation theory. The dashed line is for an identical calculation except that the $2\hbar\omega$ configurations are also treated in perturbation theory.

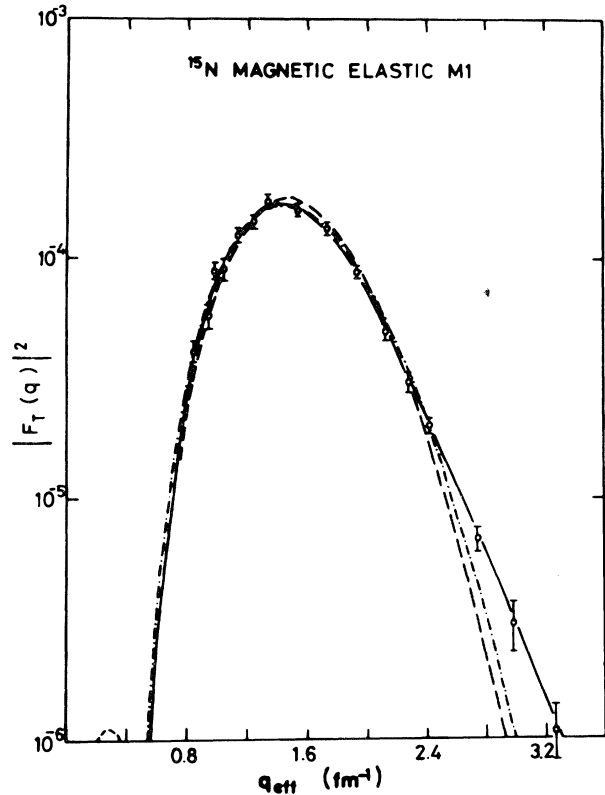


FIG. 7. Phenomenological description of the magnetic elastic form factor in ^{15}N . The $q \rightarrow 0$ limit was required to reproduce the ground state dipole moment. The dashed line is for a $0p$ shell harmonic oscillator orbital with parameters A_1 and b varied. The dotted-dashed line is for a $0p$ -shell Woods-Saxon wave function. The solid curve is obtained when terms up to x^3 are retained.

describe the elastic $M1$ scattering. Since the 6.32 MeV transition contains both $M1$ and $E2$ multipoles, we shall not attempt such an analysis of this transition because of the uncertainties in separating the various multipole contributions.

The $M1$ form factor may be expanded as follows:

$$F_{M1}(q) = \frac{\hbar c}{\sqrt{2}Mc^2Z} \mu q e^{-x} \times \{1 + A_1 x + A_2 x^2 + \dots\} F_{\text{SN}} F_{\text{c.m.}},$$

where x is proportional to q^2 and F_{SN} and $F_{\text{c.m.}}$ are the nucleon finite size and shell model center of mass corrections.¹¹ For harmonic oscillator orbitals, $x = q^2 b^2 / 4$. The magnetic moment, μ , and the coefficients A_n contain all the relevant nuclear structure information. Only terms up to order x^1 are present when consideration is limited to one-body currents within the harmonic oscillator p -shell space.

A $0p_{1/2}$ proton-hole description with bare nucleon g factors gives $\mu = -0.263 \mu_N$ and $A_1 = -7.055$ but does not provide an acceptable description of the form factor as

has been demonstrated in Fig. 1. Figure 7 shows the best fit that could be obtained by varying A_1 and b when μ is fixed at the experimental value. This is equivalent to allowing the $0p_{1/2}$ proton to have q -independent effective moments as well as an orbital size different from the value derived from the charge radius. The best parameters are $A_1 = -5.89$ and $b = 1.67$ fm. This fit describes the data well up to about 2.4 fm^{-1} , beyond which the fitted strength is insufficient to reproduce the observed magnitude. This is the best one can hope to do using harmonic oscillator wave functions within the restrictions of the $0p$ shell. The use of a Woods-Saxon wave function for the $0p$ orbital improves the best-fit χ^2 per degree of freedom from 5.5 to 3.5, but still leaves a deficiency with respect to the high- q data, as shown in Fig. 7.

Some insight into the high- q problem can be developed by increasing the order n of the polynomial expression for $F_{M1}(q)$. For example, in the harmonic oscillator model, the inclusion of an $n=2$ term introduces $2\hbar\omega$ single-particle matrix elements within the $1s-0d$ shell, and cross-shell $0p$ to $1p-0f$ contributions. Such a fit yields little improvement in the χ^2 value. The further extension of the

polynomial to include an $n = 3$ term brings into consideration $4\hbar\omega$ excitations and single-particle matrix elements within the $1p$ - $0f$ shell. In this case an essentially perfect fit is obtained, corresponding to the values $A_1 = -8.130$, $A_2 = 2.489$, $A_3 = -0.380$, and $b = 1.51$ fm.

One of the simplest configurations that will contribute to A_3 has a single nucleon in the $1p$ - $0f$ shell. For example, one might expect the dominant contribution to be

$$(0p_{1/2})^2 [J=0, T=1] \times 1p_{1/2}$$

In this case, an occupancy (amplitude squared) of 0.33 would be required to obtain the above A_3 . A similarly large admixture of the $1p_{1/2}$ orbital would also be needed to explain the large elastic $M1$ form factor observed in ^{13}C at high q .^{12,26}

VI. SUMMARY AND CONCLUSIONS

Measurements of the transverse form factors for the ^{15}N ground state and 6.32 MeV state excitation have been compared to the predictions of the $0p$ -shell proton-hole model, a $2\hbar\omega$ shell model calculation, and core-polarization models. It was found that the theoretical description of the data improved markedly as the model space was expanded. For example, the restricted $0p$ -shell model overestimated the maxima of the elastic and 6.32 MeV form factors by factors of 2 and 3, respectively. Core polarization calculations that include $12\hbar\omega$ and higher excitations provided a much more satisfactory account of the observed maxima. In common with other recently reported work,¹² the feature that is most difficult for the models to explain is the unexpectedly large cross sections measured above $q \simeq 2.4 \text{ fm}^{-1}$. The $0p$ -shell model and $2\hbar\omega$ calculations seem unable to account for these enhancements. In the case of the elastic $M1$ form factor, the evaluation of MEC effects uniformly increased the predicted form factor by about 20% over a large range of momentum transfer, but did little to remove the high- q discrepancy.

The data were compared to two different evaluations of

core-polarization contributions. The approach of the Lyon group,² which includes core-polarization effects to all orders, is considered to be more appropriate for ^{15}N than for other p -shell nuclei. As has been shown, these calculations can produce the required high- q enhancement provided that the Migdal parameter g' is chosen appropriately. The resultant $g' \simeq 0.6$ is consistent with currently accepted estimates⁴ derived from nuclear magnetic moments and other experimental evidence. On the other hand, similar calculations² by the Lyon group demanded a value of $g' = 0.44$ to explain $M1$ transitions in ^{12}C and ^{13}C . This casts doubt on the general applicability of their method.

Perturbation theory calculations of core polarization effects⁵ have also been examined. Although these calculations seem to improve upon the $0p$ -shell description, they still do not predict enough strength at high q . Similar calculations⁶ with a different interaction provide a good description of the high- q elastic data for ^{13}C , but fail in the case of the 15.1 MeV transition in ^{12}C . At present there appears to be no definite method for choosing an interaction which provides universal agreement with the transverse form factors measured for light nuclei.

By means of a phenomenological power series analysis, we have shown how core polarization effects could account for the large cross sections observed at high q . Such an explanation would require an occupancy of higher-lying orbits that is much greater than that given by customary shell model assumptions. A clear signature for the origins of the high- q discrepancy should be sought by measuring the ^{15}N and other form factors to higher momentum transfers.

ACKNOWLEDGMENTS

The authors are indebted to Professor A. Figureau and Professor T. Suzuki for their permission to include Figs. 4 and 6. One of the authors (R.P.S.) wishes to express his sincere gratitude for the generous hospitality extended to him by the Nuclear Physics Group of the University of Massachusetts at Amherst during the period of planning and execution of this experiment. Support for this work was provided by the U. S. Department of Energy.

- ¹J. Dubach, J. H. Koch, and T. W. Donnelly, Nucl. Phys. **A271**, 279 (1976).
- ²J. Delorme, A. Figureau, and P. Guichon, Phys. Lett. **99B**, 187 (1981).
- ³M. Bernheim *et al.*, Nucl. Phys. **A375**, 381 (1982).
- ⁴T. Suzuki, Ph.D. thesis, University of Tokyo, 1978 (unpublished).
- ⁵T. Suzuki, H. Hyuga, A. Arima, and K. Yazaki, Nucl. Phys. **A358**, 421c (1981).
- ⁶T. Suzuki, H. Hyuga, A. Arima, and K. Yazaki, Phys. Lett. **106B**, 19 (1981).
- ⁷G. A. Peterson, J. B. Flanz, D. V. Webb, H. deVries, and C. F. Williamson, Nucl. Instrum. Methods **160**, 375 (1979).
- ⁸F. Borkowski, P. Peuser, G. G. Simon, V. H. Walther, and R. D. Wendling, Nucl. Phys. **A222**, 269 (1974).
- ⁹W. J. Gerace and G. C. Hamilton, Phys. Lett. **39B**, 481 (1972).
- ¹⁰R. S. Hicks, A. Hotta, J. B. Flanz, and H. deVries, Phys. Rev.

C **21**, 2177 (1980).

- ¹¹T. deForest and J. D. Walecka, Adv. Phys. **15**, 1 (1966).
- ¹²R. S. Hicks, J. Dubach, R. A. Lindgren, B. Parker, and G. A. Peterson, Phys. Rev. C **26**, 339 (1982).
- ¹³M. W. S. Macauley, R. P. Singhal, R. G. Arthur, S. W. Brain, W. A. Gillespie, A. Johnston, E. W. Lees, and A. G. Slight, J. Phys. G **2**, L35 (1976).
- ¹⁴G. A. Beer, P. Brix, H.-G. Clerc, and B. Laube, Phys. Lett. **26B**, 506 (1968).
- ¹⁵J. Dubach and W. C. Haxton (unpublished).
- ¹⁶S. Cohen and D. Kurath, Nucl. Phys. **73**, 1 (1965).
- ¹⁷D. J. Millener and D. Kurath, Nucl. Phys. **A255**, 315 (1975).
- ¹⁸T. S. Kuo, Nucl. Phys. **A103**, 71 (1967).
- ¹⁹R. R. Whitehead, A. Watt, B. J. Cole, and I. Morrison, Adv. Nucl. Phys. **9**, 123 (1977).
- ²⁰G. Mairle and G. J. Wagner, Z. Phys. **258**, 321 (1973).
- ²¹R. Moreh and O. Sahal, Nucl. Phys. **A252**, 429 (1975).

²²H. Toki and W. Weise, Phys. Lett. 92B, 265 (1980).

²³J. Speth, E. Werner, and W. Wild, Phys. Rep. C33, 127 (1977).

²⁴A. Figureau (private communication).

²⁵Y. Horikawa, T. Hoshino, and A. Arima, Nucl. Phys. A278,

297 (1977).

²⁶Note that the values given in Ref. 12 for the fit parameters a_1 , a_2 , and a_3 should be multiplied by a factor of 10.2. That fit utilized a MEC-corrected value of $0.660 \mu_N$ for the ^{13}C dipole moment.